Available online at www.sciencedirect.com
SCIENCE DIRECT®
Journal of Crystal Growth 275 (2005) e1417–e1421
JOURNAL OF CRYSTAL GROWTH
www.elsevier.com/locate/jcrysgro

Melting of a DPPC lipid bilayer observed with atomic force microscopy and computer simulation

F. Yarrow*, T.J.H. Vlugt, J.P.J.M. van der Eerden, M.M.E. Snel

Debye Institute, Condensed Matter and Interfaces, Utrecht University, P.O. Box 80.000, 3508 TA Utrecht, The Netherlands

Available online 15 December 2004

Abstract

Atomic force microscopy imaging of a supported bilayer of the phospholipid DPPC revealed the presence of thin lines, which were thought to be the boundaries of domains with a different orientation. Temperature-controlled AFM showed that the melting from the gel state $L_{\beta'}$ to the fluid L_{α} phase starts on these lines. The observed onset of melting at 40.3 °C compared well to reported DSC measurements.

The same mechanism of melting was observed in computer simulations on a bilayer of a coarse-grained lipid model at the $L_{\beta'}$ phase. Two boundary lines were present in the initial configuration. It was shown that the lipid acyl tails became more disordered at the boundaries upon temperature increase.

PACS: 87.15.Aa

Keywords: A1. Atomic force microscopy; A1. Biomaterials; A1. Computer simulation; A1. Phase diagrams; B1. Biological substances

1. Introduction

In our previous study of supported, mixed peptide–DPPC bilayers, we encountered the existence of thin lines in bilayers of the pure phospholipid DPPC (1,2-dipalmitoyl-*sn*-glycero-3-phosphocholine). Small amounts of synthetic WALP peptide insert themselves into these lines. This results in a broadening [1]. It was proposed that these lines were boundaries between areas with different azimuthal tilt angles. The phospholipid DPPC is known to exhibit a range of different phases as a function of temperature (see Fig. 1). In the gel state $L_{\beta'}$ at room temperature the lipids are tilted at 33° with respect to the bilayer normal z (polar angle) [2]. However, their azimuthal angle in the bilayer plane (xy-plane) can be different [1].

Interest in the phase behaviour of these mixed peptide–lipid systems motivated us to examine the phase properties of pure DPPC bilayers on mica. Although the phase transitions have been extensively investigated with techniques like differential scanning calorimetry (see, for instance, Ref. [3]),

*Corresponding author. Fax: +31 30 2532403.
E-mail address: f.yarrow@phys.uu.nl (F. Yarrow).

0022-0248/$ - see front matter © 2004 Published by Elsevier B.V.
doi:10.1016/j.jcrysgro.2004.11.237

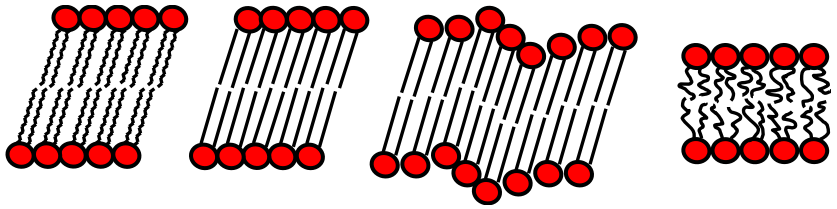

Fig. 1. Different phases of DPPC. From left to right: the sub-gel phase $L_{c'}$, the gel-state phase $L_{\beta'}$, the ripple phase $P_{\beta'}$ and the high-temperature fluid L_{α} phase. The ordering of the acyl tail-chains decreases from the left to the right. A DPPC molecule consists of a hydrophilic head (red) and two hydrophobic tails (black). The hydrophilic head sticks in the water (not shown here).

the unique capabilities of the AFM to image the topography during melting have not been explored in many studies. Tokumasu et al. [4] have observed melting of a supported DMPC bilayer from the $L_{\beta'}$ to the L_{α} phase with tapping mode AFM, while increasing the temperature continuously. However, they did not observe any boundary lines. In this study, we use temperature-controlled AFM on pure DPPC bilayers to show that melting starts at these borders. Furthermore, we have performed Dissipative Particle Dynamics (DPD) computer simulations on a bilayer with two boundary lines. These results correlate qualitatively to the experimental AFM data.

2. Methods and materials

2.1. AFM

The phospholipid DPPC was purchased from Avanti Polar Lipids Inc. with a purity >99%. A solution containing DPPC vesicles in 20 mM NaCl was made with the vesicle fusion protocol [1]. We then applied this solution to freshly cleaved mica (Structure Probe Inc.) and heated for 45 min at 60 °C, while keeping it hydrated. The mica with the bilayer was placed on the AFM after washing and cooling to room temperature. The temperature was then changed in steps by use of a heating sample stage (Molecular Imaging) connected with a Lakeshore Temperature Controller 330. Images of the sample were recorded when the temperature reached a steady value.

Imaging was performed in 20 mM NaCl in contact mode with a PicoScan Atomic Force Microscope (Molecular Imaging). Si_3N_4 cantilevers (Digital Instruments Inc.) with a spring constant of 0.06 N/m (manufacturer's specifications) were used. The scanning force was adjusted to the lowest possible value that allowed stable imaging. Care was taken to use approximately constant scanning forces during the temperature sweeps to allow comparison of the images.

The temperature on top of the mica sample was checked afterwards with a Pt-100 thermometer with a measuring area of 1.2 mm^2 (Type GW 2105, Sensycon). We found that the temperature on top of the sample deviated from that given by the temperature controller, which measures underneath the sample stage. The average of the measured temperatures is used here. The actual temperatures were found to fluctuate up to 0.4 °C around these mean values, depending both on time and position on the sample stage.

2.2. Computer simulation

We have studied the experimentally observed phase transition using molecular simulations. Conventional molecular simulation techniques such as Monte Carlo or molecular dynamics often employ all-atom models in which each atom of the system (lipid bilayer and water) is modelled as a single particle. Although these simulations are possible on modern computers [5], they are still too time-consuming to study phase transitions. Therefore, we have used a coarse-grained mesoscopic model based on DPD [6,7] that leaves out many of the chemical details of the water and the lipids but still is able to capture the essential aspects of the phase behaviour. We refer the reader to Refs. [8–10] for details concerning the model and simulation methodology.

The phase behaviour of this system strongly depends on the interactions between the hydrophilic head groups and on the temperature. At low temperature, the stable phase is the so-called sub-gel phase L_c' in which the tails are ordered and tilted in one direction. For the head–head interaction used in this study, the pre-melting transition from the L_c' to the L_β' phase takes place at a reduced temperature of $k_BT = 0.3$ in which k_B is the Boltzmann constant [9,10]. In this so-called L_β' phase, the tails are still tilted but less ordered, see Fig. 1. It is important to note that the temperatures in the DPD simulations cannot be compared directly with the temperatures in the experimental system. However, we can still make a more qualitative comparison of the system below the transition temperature.

3. Results and discussion

3.1. AFM

The topography of a DPPC layer on mica near room temperature is shown in the AFM image in Fig. 2a. The image shows a uniform, flat layer without any apparent features. The height of this layer was 5–6 nm, which was measured through spontaneously arising holes (not shown). This confirms the presence of a single, hydrated bilayer with a water layer between the mica and the lipid bilayer [11].

A darker, lower line is observed. Such lines are commonly observed in these layers and are thought to be boundaries between areas with a different tilt direction [1]. Different areas will form at the cooling step during sample preparation, where the lipid crystallizes from the non-tilted, disordered liquid crystalline phase L_α to the tilted gel phase L_β'. Growth of the L_β' phase will begin at different locations throughout the sample. Boundaries are formed where these areas meet, as the domains will have different azimuthal angles while having the same polar angle of 33° [1]. Note that the intermediate ripple phase P_β' is not observed in supported, unilamellar bilayers [12].

An increase in the temperature clearly shows the onset and growth of a second, lower phase in Figs. 2b–f. The height difference Δh between the coexisting phases is 0.7–1.5 nm, depending on details of the exact measuring force used. The lower phase consists of the fluid L_α phase, for which a Δh of 1 nm can be found in the literature compared to the gel phase [1]. The force of the scanning tip probably compresses the L_α phase somewhat, yielding a larger value for Δh.

The melting starts at 40.3 °C and the phase transition is complete at 43.0 °C. A differential calorimetry scanning (DSC) study on DPPC vesicles showed an onset of the endothermic peak of the main transition at 40 °C and its maximum at 41.5 °C [13]. It was also shown that supported DPPC bilayers on mica essentially show the same phase behaviour, with a peak at 40.4 °C [14]. This seems to compare reasonably well with our results.

It is important to note that Fig. 2 clearly reveals the melting mechanism of melting is revealed. The fluid phase initially only appears at the boundary lines, from where it continues to grow.

3.2. Computer simulation

We started our simulation with a bilayer (xy-plane) at low temperature ($k_BT = 0.2$) in the L_β' phase. The tails of the bilayer are tilted in the yz-plane; see Fig. 3. Two different lipid domains are generated by choosing an azimuthal angle $\varphi = \pi/2$ outside the region between $0.25B_x$ and $0.75B_x$ and $\varphi = -\pi/2$ inside that region. B_x is the size of our simulation box in the x-direction. This system was simulated at the phase transition to L_β'. At temperatures below $k_BT = 0.26$, the domain boundaries were stable. However, at $k_BT = 0.30$, we found that the domain boundaries disappeared spontaneously, see Fig. 3. The interesting point is that the preferred tilt direction has changed from the yz-plane to the xz-direction. Apparently, this change is easier for the system that reverting back one of the domains.

The observed change in tilt direction in the simulations as well as the experimental AFM images suggests that the melting transition starts at the domain boundaries. To test this hypothesis, we have introduced a parameter d, which measures the average closest distance between hydrophobic beads and a fictitious line connecting the first and

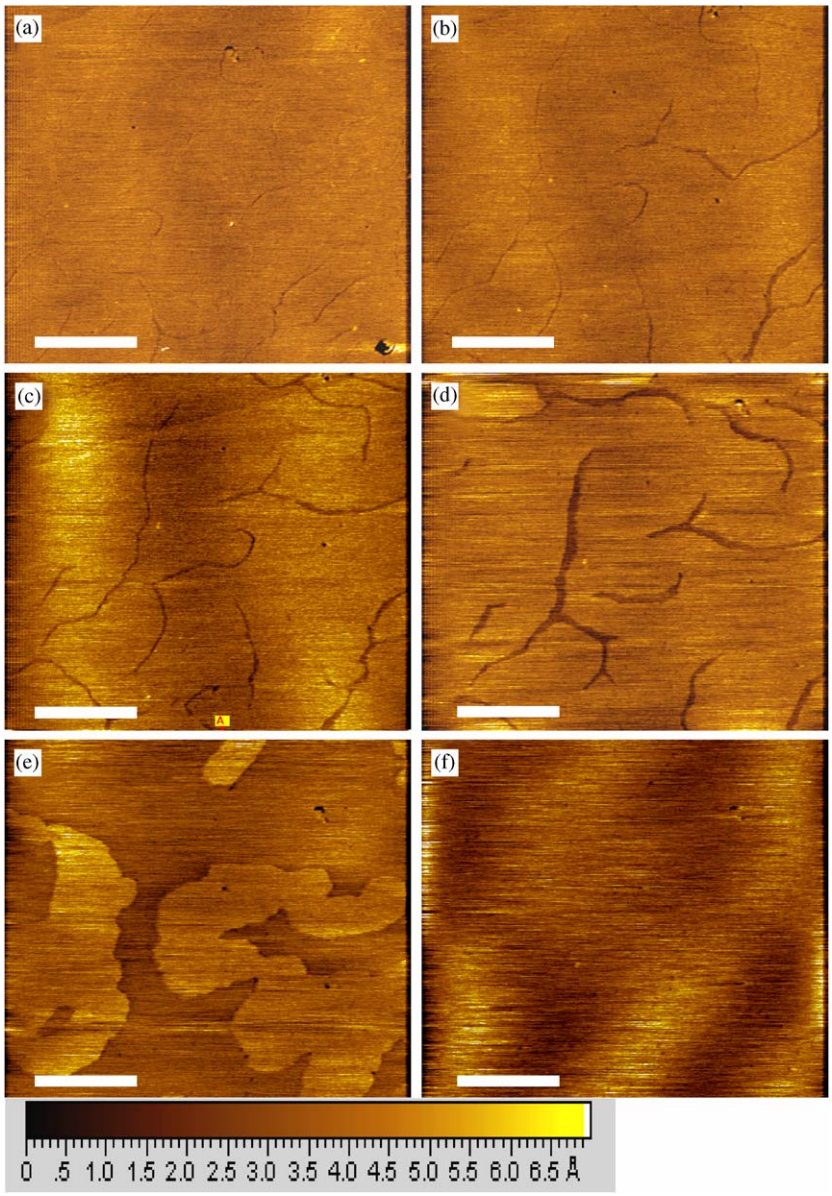

Fig. 2. AFM height images of a single area of the DPPC bilayer at different temperatures: respectively 24.7 °C (a), 40.3 °C (b), 40.8 °C (c), 42.0 °C (d), 42.7 °C (e) and 43.0 °C (f). The scale bar is 750 nm. A higher area is represented by a lighter colour.

last hydrophobic bead of a lipid tail. A large value of d indicates that the tails are more flexible. In Fig. 4, we have plotted the average order parameter d as a function of the location in the bilayer. Clearly, this order parameter is large around the domain boundaries, suggesting that the melting transition starts here.

One should keep in mind that the simulation results are hindered by periodic boundary conditions as well as relatively small system sizes and

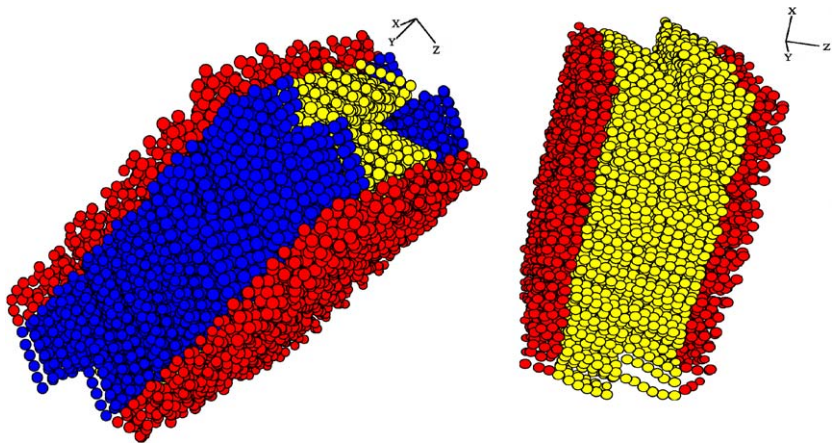

Fig. 3. DPD simulations of a lipid bilayer at $k_{\underline{B}}T = 0.30$ Left: Starting configuration of our lipid bilayer. There are two domains, in which the azimuthal tilt angle is reversed. The reverted domain is coloured blue. The domain boundaries are located in the *yz*-plane. Right: Final configuration. For clarity, we have omitted the water in both configurations. The hydrophilic beads are colored red.

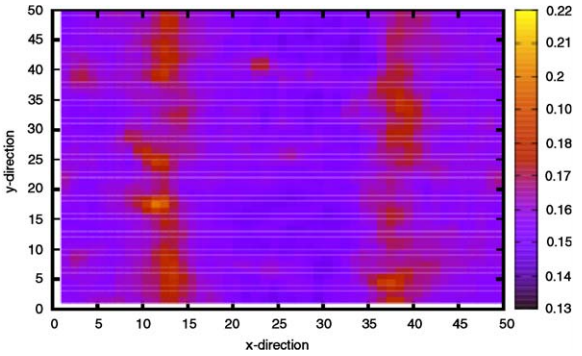

Fig. 4. Order parameter d describing the flexibility of the lipid tails as a function of the relative position (range: 0–50) in the bilayer at $k_B T = 0.30$.

therefore the lipids may change their tilt-plane more easily in the model than in the experiment.

4. Conclusion

Melting of a supported DPPC bilayer can be observed with temperature-controlled AFM. The melting starts preferentially along the boundary lines between areas with a different tilt direction (azimuthal angle). DPD computer simulations on a coarse-grained model support this mechanism, where an increased disorder is observed at the boundaries.

References

[1] H.A. Rinia, R.A. Kik, R.A. Demel, M.M.E. Snel, J.A. Killian, J.P.J.M. van der Eerden, B. de Kruijff, Biochemistry 39 (2000) 5852.
[2] D. Marsh, in: Handbook of Lipid Bilayers, CRC Boca Raton, USA, 1990.
[3] R. Koynova, M. Caffrey, Biochim. Biophys. Acta 1376 (1998).
[4] F. Tokumasu, A.J. Jin, G.W. Feigenson, J.A. Dvorak, Ultramicroscopy 97 (2003) 217.
[5] S.J. Marrink, D.P. Tieleman, J. Am. Chem. Soc. 123 (2001) 12383.
[6] P.J. Hoogerbrugge, J.M.V.A. Koelman, Europhys. Lett. 19 (1992) 155.
[7] R.D. Groot, P.B. Warren, J. Chem. Phys. 107 (1997) 4423.
[8] M. Venturoli, B. Smit, Phys. Chem. Commun. 10 (1999) 1.
[9] M. Kranenburg, M. Venturoli, B. Smit, J. Phys. Chem. B 107 (2003) 11491.
[10] M. Kranenburg, M. Venturoli, B. Smit, Phys. Rev. E 67 (2003) 060901.
[11] L.K. Tamm, Z. Shao, in: P.I. Harris, D. Chapman (Eds.), Biomembrane Structures, IOS Press, Amsterdam, 1998, pp. 169–185.
[12] C. Leidy, T. Kaasgaard, J.H. Crowe, O.G. Mouritsen, K. Jørgensen, Biophys. J. 83 (2002) 2625.
[13] H.A. Rinia, Atomic Force Microscopy on domains in biological model membranes, PhD thesis, University Utrecht, 2001.
[14] J. Yang, J. Appleyard, J. Phys. Chem. B 104 (2000) 8097.